Numerical Optimization of a Trapezoidal Labyrinth Seal for Pulsed Compression Reactor (PCR)

Hermann E, Alcázar, PhD[1], Briam R. Velasquez, BS[1], César P. Castillo, MSc[1], and Leopoldo O. Alcázar, PhD[1]

[1]Universidad Catolica de Santa Maria, Perú, hermannalcazar@ucsm.edu.pe, 72099424@ucsm.edu.pe, ccastill@ucsm.edu.pe, lalcazar@ucsm.edu.pe

Abstract*– A sealing system using labyrinth seal is proposed to minimize gas leaks in a Pulsed Compression Reactor, for which the geometric parameters of trapezoidal shape are evaluated. The set of parameters was optimized by minimizing gas leaks, using the Multiobjective Genetic Algorithm with the Genetic Aggregation method, which performs a regression model with the data generated by the correlation of parameters. The CFD simulation evaluates gas leakage for the given geometry and constant boundary conditions, inlet pressure 10 MPa, piston velocity 25 m/s, 35° cavity angle and 150 mm piston length. The values in the input set have been reduced to manufacturable quantities. The analysis of the velocity behavior shows a sudden increase in velocity in the final part of the cavity, and consequently, the turbulence kinetic energy presents peaks in that area. The most sensitive parameters are the gap between the piston and cylinder, and the width of the cavity. The minimum flow leakage is 0.001024 kg/s with a gap of 30 µm. When comparing between the smooth and grooved piston, there are regions where having a smooth surface is better than grooving it. In general, over a threshold gap-value of 150 µm is better to use a piston with labyrinth seals. For a gap of 250 µm the leakage flow was 0.301391 kg/s this represents a decrease of 34% compared to a smooth piston.

Keywords—Trapezoidal labyrinth seals, pulsed compression reactor, CFD simulation, Ansys Fluent.

I. Introduction

The main objective of this study is the parameter's optimization of a Pulsed Compression Reactor (PCR) trapezoidal labyrinth seal, in order to minimize the leakage for a piston speed of 25 m/s and methane pressure of 10 MPa.

A. Pulsed Compression Reactor (PCR)

A PCR is a piston–cylinder device where reaction at high temperature and pressure takes place at the cylinder chamber. This system presents two main characteristics. The piston travels at high speeds, compressing the gas within the chamber, [1], [2]. This produces an instantaneous thermodynamic process (adiabatic), which allows the production, within other applications, of amorphous nanoparticles. First, the chamber is filled with the gas, after which the piston is moved at high speed, generally using a pressurized inert gas (nitrogen or helium), loaded in the second chamber, Fig. 1. Some advanced applications, [1], used the same compressed gas to move the piston backward.

Initially, PCR-related researches were carried out indirectly, as in the case of the ballistic compressor [3] that has similarities with this type of reactor. The use of non-contact seals in internal combustion engines has been studied widely, [4], [5], [6], [7], [8], [9], [10], [11], [12], [13], [14], however the use of oil lubricant contaminates the reaction chamber, methane gas in this application. In addition, the working pressures with which it works are low compared to the pressures that are expected to have in this work.

Digital Object Identifier (DOI):
http://dx.doi.org/10.18687/LACCEI2021.1.1.347
ISBN: 978-958-52071-8-9 ISSN: 2414-6390

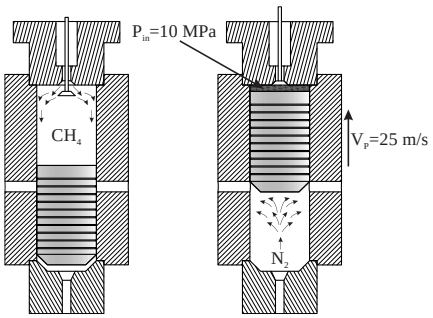

Fig. 1 Pulsed Compression Reactor (PCR).

Thus, effective oil-free PCR sealings were studied by [15] and [16]. Three major advantages of PCRs are non-gas contamination due to oil, no wear due to non-contact seals, and theoretically unlimited service life, [17].

B. PCR Labyrinth Seal

A labyrinth seal is a system with several cavities on the piston surface, where the fluid is forced to circulate through them. In each of the cavities, turbulence is generated increasing the wall friction, dissipating the kinetic energy thus reducing the leakage flow. Labyrinth seals are suitable to be used with high-speed pistons and high compression pressures, [15]. During the design process, considerations must be made to guarantee enough free space between the piston and cylinder walls, [17].

Since 1935 [18] many compressors were equipped with labyrinth seals. Since then, several calculation methods of labyrinth seals were developed, [16], [19], [20], [21], [22], [23]. Currently, researchers are focused on the study of thermodynamic effects, numerical (CFD) and theoretical modelling, and leakage visualization and measurement.

To achieve adiabatic compression, the piston shall move freely at speeds between 5-40 m/s, [1]. The cycle period should not exceed 0.01 seconds [24], which minimizes the heat exchange between the gas and the piston and cylinder walls.

A previous work, [25], presented a numerical analysis of the behaviour of PCR labyrinth with triangular, quadrilateral,

and trapezoidal shapes. A comparison between them concluded that seals with trapezoidal cavities have lesser leakage. The cavity angle of 35° is the one that produces the higher energy loss, due to the formation of vortices at the inlet and outlet of the cavities.

The objective of this study is the optimization of a trapezoidal labyrinth for PCR applications. This pulsed compression reactor is intended to be used to produce carbon nanoparticles, [26], after an adiabatic decomposition of methane into hydrogen and carbon nanoparticles, carbon nanotubes, or graphene.

II. METHODOLOGY

A. *Geometry*

The geometric parameters needed to define completely a trapezoidal shape are indicated in Fig. 1. These parameters are: piston diameter, length (d, L), gap between piston and cylinder (G), initial and final free length (J_{in}, J_{out}), cavity length, depth, angle (W, H, α), and distance between cavities (e).

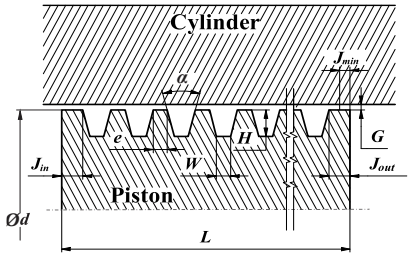

Fig. 2 Geometry definition for trapezoidal shape.

For this study, some parameters were fixed. The piston diameter, piston length, cavity angle, initial free length, and minimum final free length are stated as constant parameters, Tab. 1. Variable parameters are to be optimized minimizing the gas leakage. The gap piston-cylinder, cavity length, cavity depth, and distance between cavities are the four variable parameters, Tab. II. The limiting values were selected according to manufacture considerations.

TABLE I
TRAPEZOIDAL CONSTANT PARAMETERS

Piston diameter d (mm)	Piston length L (mm)	Cavity angle α (°)	Initial free length J_{in} (mm)	Minimum final free length J_{min} (mm)
60	150	35	10	10

TABLE II
TRAPEZOIDAL VARIABLE PARAMETERS

Gap piston-cylinder G (μm)	Cavity length W (mm)	Cavity depth H (mm)	Distance between cavities e (mm)	Final free length J_{out} (mm)
30 - 250	0.5 – 10.0	0.5 – 10.0	0.5 – 10.0	$> J_{min}$

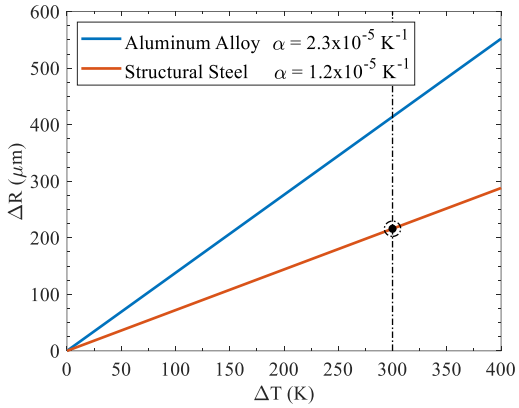

Fig. 3 Piston radial increase due to temperature change.

The temperature of the gas after compression is expected to increase significantly. Some studies estimate the reaction temperature at 1000 K. Due to radiant and convective heat transfer, the piston temperature in internal combustion engines, increases about 30% of the combustion temperature. In this case is expected a piston temperature change of 300 K. For a piston diameter of 60 mm, a change in temperature of 300 K results in a radius increase of 200 μm for a steel piston, Fig. 3. For aluminum piston the radial increment almost doubles.

The piston temperature is time and length dependant. Initially, the piston temperature will be uniform, closely to temperature. After some time working, the piston side at the reaction chamber will be close to 300 K, while the other side remains cool. This means that the gap between piston and cylinder will be reduced in 200 μm through the working time. For this reason, a sensitivity study for a gap from a minimum of 30 μm to a maximum of 250 μm is performed, Tab. II.

B. *Numerical Simulation*

The numerical simulation was developed using ANSYS Workbench. Three steps were carried out. Firstly, the geometry/mesh generation, then the model simulation, and finally compute leakage mass flow, as shown in Fig. 4.

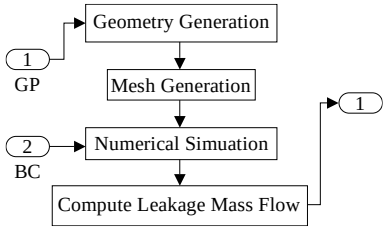

Fig. 4 Fluid Flow Simulation Subsystem.

Since the values of the parameters change for each analysis, a parametric CAD model was considered. The ANSYS SpaceClaim Direct Modeler program was used, within ANSYS Workbench, which allows the creation of CAD

models using the programing language Python. All the parameters, constants, and variables are parametric input data. The geometry returned by the script is a 2-D axisymmetric shape that represents the fluid domain. The geometry was virtually sectioned, these cuts do not mean physical meaning, such as whether there is a wall, conditional surface interchange, etc. The reason is that the area can be better meshed (multi-block structure grid).

Once the geometry is generated, then it is meshed. If the mesh is too big, convergence and accuracy problems are likely to have. Meshing is made up of a discrete number of points, which overlap the entire geometry of the domain. By subdividing the area, many grids or smaller grid cells can be generated [27]. The criteria to generate the meshing were: aspect ratio, Orthogonal Quality (Orthogonal Quality) O.Q. ≈ 1, and the dimensionless distance to the wall y+ ≈ 30-300. Taking this into account, the meshing was carried out using a multi-block structure grid with matching cell faces. These mostly quadrilateral elements and a minority of triangular elements, taking as a base element size of 20 µm, for the radial space between the cylinder and the piston (gap), performed an Edge sizing with divisions of 30 with a bias that has a factor of 3, for a pattern of accumulation of elements at the ends in the inlet, and outlet.

The fluid flow simulation was performed in ANSYS Fluent. For this, it was configured as axisymmetric analysis and based on pressure. ANSYS Fluent Theory Guide recommends the use of a Realizable k-epsilon viscosity model when the fluid includes vortices, [28]. Better results were obtained when compared with k-epsilon and k-omega models. Other necessary simulation parameters are indicated in Tab. III.

TABLE III
ANSYS FLUENT PARAMETERS

Gas model	Turbulence Model	C_2	σ_k	σ_ε
Ideal gas (piecewise-polynomial)	Realizable k-ε	1.9	1.0	1.2

The boundary conditions introduced to the model are shown in Tab. IV. The gas is methane, and its pressure is 10 MPa. The piston speed is set to 25 m/s and the outlet pressure is atmospheric.

TABLE IV
MODEL BOUNDARY CONDITIONS

Gas	Inlet BC	Outlet BC	Piston speed
Methane, **CH_4** (compressible gas)	**10 MPa @**300 K	Atmospheric 0 MPa @300 K	**25 m/s**

The way in which the boundary conditions were placed was modified since it was observed that the simulation did not converge. This is due to the fluid becoming supersonic within the labyrinth seals, reaching values around Mach equal to 1.2. Then a parameter called "Supersonic/Initial Gauge Pressure" was added, defining it as 0.95 times the inlet pressure 10 MPa. In addition, the restriction of "Prevent Reverse Flow" was added. The simulation was initialized using “Standard Initialization” based on the Boundary Condition (BC) of the input.

The number of iterations for each simulation was set to 2000. In the previous study [26] it was set to 1500. This change is because a greater range was studied for the parameters and there were settings in which convergence was not reached with 1500 iterations, that is why the quantity was increased.

C. Parameters Correlation and Optimization

The parameter correlation and optimization block diagram are shown in Fig. 5. This includes the search for parameter sensitivity and then continues with the search for a suitable regression model for the data generated by the parameter correlation. The optimization of the geometric parameters is then carried out based on the mathematical model created. It was established that there are three optimal candidates, which were taken to a verification. That is, a numerical simulation was performed for each candidate. If the difference between the leakage mass flow value provided by the mathematical model and the numerical simulation is less than 5%, the optimization process ends; otherwise, the optimization process continues. On the contrary, if this criterion is not met, the candidate value is added to the data and a new regression model is found again. And the optimization is completed again.

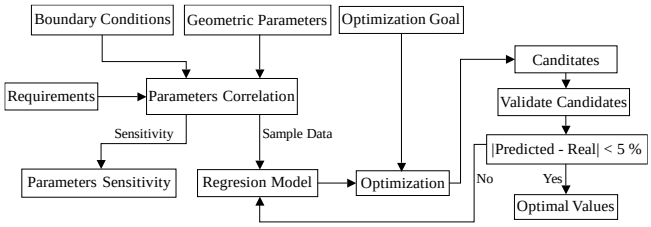

Fig. 5 Parameter correlation and optimization block diagram.

The parameter correlation analysis was performed to find the sensitivity of the geometric parameters, which defines the influence of the design parameters on the leakage mass flow. The higher the sensitivity factor, the greater the impact. For the generation of the samples, the Spearman method was used. The requirement to perform the analysis was defined by the number of samples, with a value of 400. These samples were restricted following the limit values defined in Tab II. The procedure to obtain the sensitivity of the parameters is shown in Fig.6.

To determine a mathematical model of the leakage mass flow based on the selected geometric parameters, the method of Genetic Aggregation was used. This method automates the process of selecting, configuring, and generating the type of response surface that best suits each output parameter of the problem. From the different types of response surfaces available within ANSYS (second-order complete polynomials,

nonparametric regression, Kriging, or moving least squares), genetic aggregation automatically creates the type of response surface that is the most appropriate approach for each output [28].

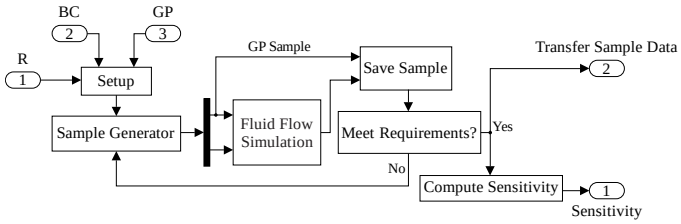

Fig. 6 Parameter correlation and optimization block diagram.

The optimization of the geometric parameters, having as a cost function the minimization of the leakage mass flow, was carried out using the Multiobjective Genetic Algorithm (MOGA). This algorithm is a hybrid variant of the popular NSGA-II (non-dominated ordered genetic algorithm-II) based on concepts of controlling elitism. Supports all kinds of input parameters. The Pareto classification scheme is performed using a rapid, non-dominated classification method that is an order of magnitude faster than traditional Pareto classification methods [29]. 800 samples were defined per iteration and a maximum of 20 iterations. The Maximum Allowable Conditions of Pareto MAPP Percentage and CSP Convergent Stability Percentage were set at 70% and 2%, respectively.

III. Results

After performing the parameter correlation analysis, the results obtained from the sensitivity of the parameters as a function of the leakage mass flow are synthesized in Fig. 7. Can be seen that the gap between piston and cylinder is the most sensitive, with a sensitive value of 0.96 over 1.00. The sensitivity for the distance between cavities, cavity width, and cavity depth are 0.14, 0.31, and 0.23, respectively. This indicates that in importance, the distance between cavities has a third of the gap but doubles the depth. The width is 60% more sensitive than the distance between cavities. The coefficient of determination of the quadratic regression R2 of the leakage mass flow obtained was 0.97.

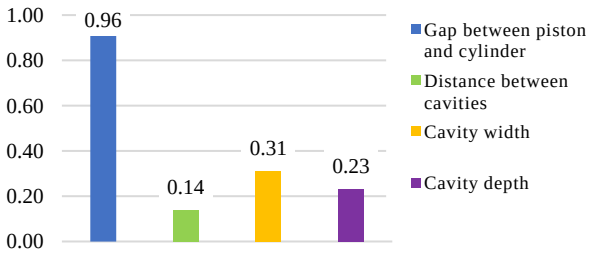

Fig. 7 Parameter's sensitivity.

For the whole domain, the minimum flow leakage is 0.01024 kg/s, Tab. V. As expected from the high dependence of the gap, this minimum value is obtained from the minimum gap value of 30 μm.

TABLE V
Minimum Absolute Mass Flow Leakage

Gap piston-cylinder ***G*** (μm)	Cavity length ***W*** (mm)	Cavity depth ***H*** (mm)	Distance btw. cavities ***e*** (mm)	Mass flow leakage (kg/s)
30	0.5	0.5	10.0	0.01024

For the given values in Tab. V, an evaluation of the leakage mass flow is done varying the gap and one of the other three parameters, depth, length, and distance between cavities. Maintaining constant two of the cavity's parameters, for the values given in Tab. V, a surface fitting was obtained. This approximate mathematical model was obtained using the Ansys Response Surface Type's Genetic Aggregation method. The value of the surface response reliability or stability was set to be between 1-0.99, and the quality of interpolation was 0.79.

A. *Variation of the distance between cavities*

The leakage mass flow surface is obtained varying the gap between piston-cylinder and the distance between cavities, maintaining constant the minimum values of the depth in 0.5 mm, and length in 0.5 mm, Fig. 8. As seen, the gap is highly sensitive.

Over the fitted surface has also been plotted the surface for a smooth piston, i.e., when the piston has no cavities. The smooth piston surface is plotted in red and only in the event when leakage is higher than with labyrinth seals. It indicates that is better the use of labyrinth seals for values above the threshold line.

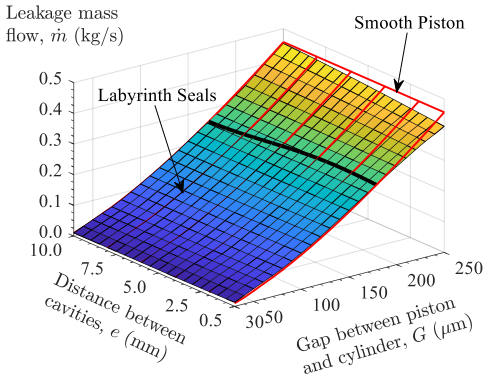

Fig. 8 Leakage vs gap and distance btw. cavities, for minimum values.

B. *Variation of the width*

Similar to Fig. 8, in Fig. 9 the leakage mass flow surface is obtained varying the gap and the cavity width. The other

two parameters are kept constants to the minimum values of the depth in 0.5 mm, and distance between cavities in 10 mm.

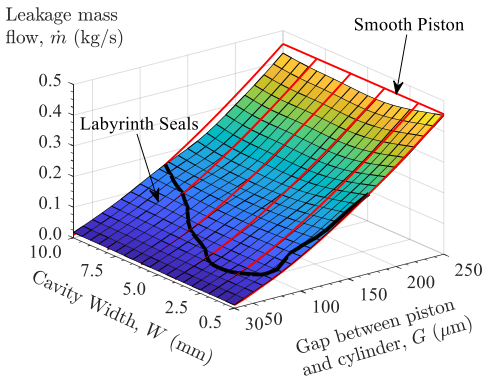

Fig. 9 Leakage vs gap and cavity width, for minimum values.

C. *Variation of the depth*

Similar to Fig. 8 and Fig. 9, in Fig. 10, the leakage mass flow surface is obtained varying the gap and the cavity depth. The other two parameters are kept constants to the minimum values of the width in 0.5 mm, and distance between cavities in 10 mm.

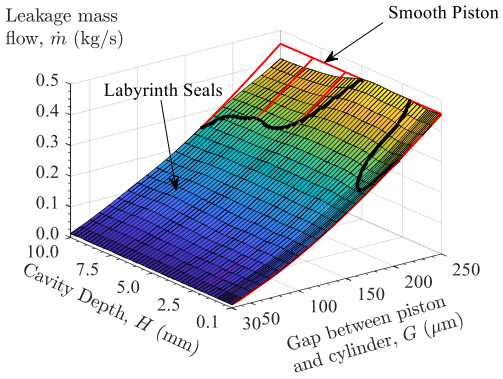

Fig. 10 Leakage vs gap and cavity depth, for minimum values.

D. *Comparison of width, depth, and distance btw. cavities*

A threshold limit existence is indicated in Fig. 11 for the width, depth, and distance between cavities. This threshold separates the two regions, where is best the use of a smooth piston or a piston with labyrinth seals. The leakage mass flow is the target value that indicates which is better, the lower the value the better option. These two zones were also studied and evidenced by [15] and [30].

The main parameter that states the use of a smooth or grooved piston is the gap between the piston and cylinder. For the distance between cavities parameter, the threshold has a gap-value of 180 µm, over the whole distance domain.

For small values of cavity width or depth, this threshold dissipates for a smooth piston as the best sealing mechanism. For values above 8 mm, the threshold gap-value is around 150 µm. In between, the threshold gap-value reduces for the width and increases for the depth. This behavior must be taken into account for the final design of the piston cavities.

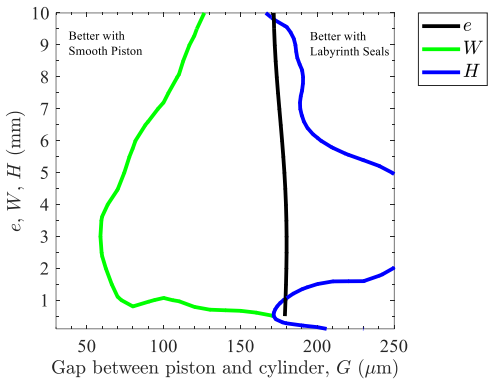

Fig. 11 Threshold between smooth and piston with labyrinth seals.

IV. Sealing Mechanism

The sealing mechanism is due to the pressure drop along the piston-cylinder gap and cavities. To understand this mechanism, first, a velocity contour analysis was performed at the last cavity, Fig. 12. At the cavity inlet, the gas enters through the gap, expanding abruptly reducing its speed. It generates a vortex at the cavity center (zero velocity), moving the gas around this vortex. Seems that it works like a vortex or damper of the incoming gas.

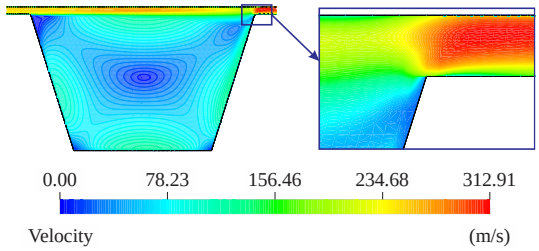

Fig. 12 Velocity contour.

At the cavity outlet, a reduction in the cross-sectional area increases its speed. This speed is highly influenced by the gap and piston speed. The velocity reaches a value of 312 m/s, just below the speed sound (343 m/s), in a turbulent regime. The gas speed at the outlet is higher at the cylinder wall than the piston wall, almost double. Is expected that heat exchange through the cylinder wall will be higher than through the piston wall.

For a 250 µm piston-cylinder gap, a mass flow leakage analysis was performed, Tab. VI. Optimum parameters were

set to be 0.5 mm, 9.5 mm, and 2.4 mm for the distance, length, and depth, respectively. For these parameters, the mass flow leakage is 0.301391 kg/s, and for a smooth piston in 0.456771 kg/s. A reduction in 34% in gas leakage is seen when labyrinth seals are used, compared to a smooth piston.

TABLE VI
MINIMUM MASS FLOW LEAKAGE COMPARISON, 250 μm Gap

Parameters	Labyrinth Seals	Smooth Piston
Gap piston-cylinder, ***G*** (μm)	250	250
Distance btw. Cavities, ***e*** (mm)	0.5	
Cavity Length, ***W*** (mm)	9.5	
Cavity Depth, ***H*** (mm)	2.4	
Mass Flow Leakage, (kg/s)	0.301391	0.456771

The turbulence kinetic energy and the pressure drop along the piston were evaluated for a 250 μm piston-cylinder gap, Fig. 13 and Fig. 14, respectively. The parameters data are the optimum values indicated in Tab. VI. In both figures, a comparison with a smooth piston is shown.

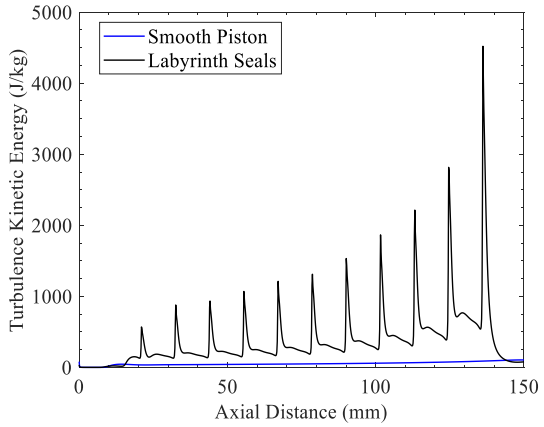

Fig. 13 Turbulence kinetic energy along the piston, 250 μm gap.

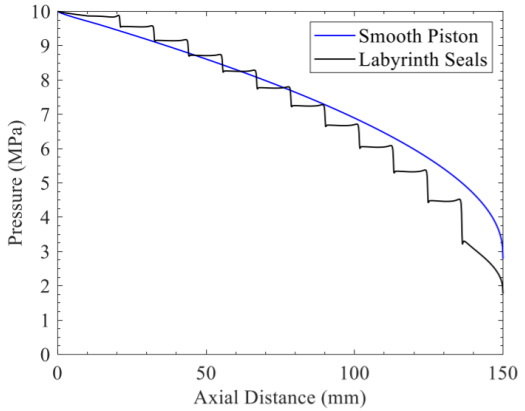

Fig. 14 Pressure drop along the piston, 250 μm gap.

The turbulence kinetic energy for labyrinth seals has peak values at the outlet of each cavity. These peaks have a direct correspondence with the speed increase indicated previously. The length of the peaks is smaller than the distance between cavities, which is an indicator that this distance could be reduced to maintain almost invariant the leakage. The largest peak is developed at the end of the last cavity, and is 18 times greater than the maximum value reached by the smooth piston.

An increase in the pressure drop is seen at the outlet of each cavity, similar behavior to the turbulence kinetic energy, as stepped jumps. For the smooth piston, the pressure drop increases linearly at the first 75% of the piston length, decreasing exponentially at the final 25%. From 0 to ~50 mm of the piston length, the smooth piston pressure drop is higher than the piston with labyrinth seals. From this ~50 mm gap, the behavior is reversed, and the pressure drop jump at each cavity increases.

V. OPTIMAL VALUES

Finally, a parameter optimization was performed for discrete gap values of 50, 100, 150, 200 and, 250 μm. In Fig. 15 the optimal values for each parameter are shown, obtained after minimizing the mass leakage flow. It is observed that in the case of "e" there is a value of 10 mm for the cases of 30 and 50 um of the gap and then it drops suddenly to values that range between 0.5 and 1 mm for the other gaps evaluated. This is due to the little influence that "e" has on these gap values. In the case of "W", it is observed that it grows together with the gap values, reaching 9.5 for a gap of 250 μm. In the case of "H" for values between 30 and 100 μm it fluctuates between 0.2 and 2 mm, after which it presents an increasing behavior until it reaches a value of 2.4 mm.

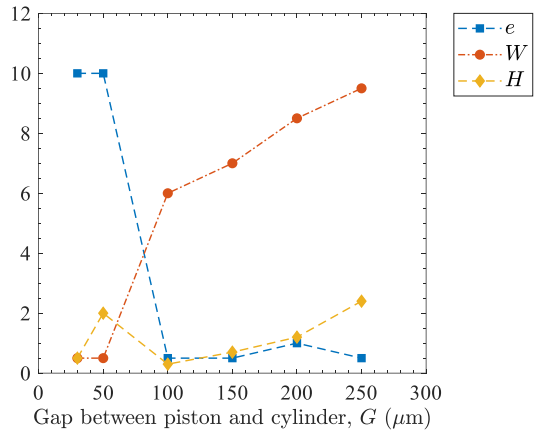

Fig. 15 Optimum values of distance btw. cavities, cavity width, and cavity depth for different values of gap.

VI. CONCLUSIONS

The numerical optimization of a trapezoidal labyrinth seal for a pulsed compression reactor was carried out successfully. For a 60 mm piston diameter, 150 piston length, 25 m/s piston speed, 35° trapezoidal cavity angle, and methane gas at 10 MPa as the fluid source, a set of geometric parameters as the gap between piston and cylinder (30-250 μm), cavity length (0.5 – 10.0 mm), cavity depth (0.5 – 10.0 mm), and distance between cavities (0.5 – 10.0 mm), were optimized.

The gap is the most sensitive parameter with a value of 0.96, and sensitivities for the distance, width, and depth of 0.31, 0.23, and 0.14, respectively. Was evaluated a threshold that separates two regions where is best the use of smooth piston or a piston with labyrinth seals. Overall, is best the use of piston with labyrinth for gap values over 150 μm.

The leakage mechanism was also analysed. A high increment in the gas speed at the outlet of the trapezoidal grove, over the gap at the distance between cavities zone, has a direct correlation with a peak increment of the turbulence kinetic energy and a stepped increment of the pressure drop.

For a gap of 250 μm, a reduction in 34% in gas leakage is seen when labyrinth seals are used, compared to a smooth piston. Optimum parameters for this analysis were set to be 0.5 mm, 9.5 mm, and 2.4 mm for the distance, length, and depth, respectively.

ACKNOWLEDGMENT

We would like to thank the Mechanical Engineering Department Chair and the Research Vice-President of the Universidad Católica de Santa María from Perú, for their support in the development of this work.

REFERENCES

[1] A.-E. C. Kronberg, Technology Report: Pulsed Compression Reactor. *Creatieve Energie*, 2008

[2] M. Glouchenkov, A. Kronberg, and H. Veringa, "Free piston pulsed compression reactor," *Chemical Engineering Transactions*, vol. 2, 983-988, 2002.

[3] P. A. Longwell, H. H. Reamer, N. P. Willburn, and B. H. Sage, "Ballistic piston for investigating gas phase reactions," *Industrial & Engineering Chemistry*, vol. 50, 603-610, 1958.

[4] Y. A. Kolbanovskiy, "Pulsed compression of gases in chemistry and technology," *Impulsnoye szhatiye gazov v khimii i tekhnologii*, USSR, 1982.

[5] P. W. Morrison Jr. and J. A Reimer, "Silane pyrolysis in a piston reactor," *AIChe Journal*, vol. 35, 793-802, 1989.

[6] L. Von Szeszih, "Herstellung von Synthesegas im Otto-Motor bei gleichzeitiger Arbeitsgewinnung," *Chemie Ingenieur Technik*, vol. 28, 190-195, 1956.

[7] B. J. Jan, W. J. Van Dijck, and B. Johannes, *United States Patent* Nº 2814551A, 1957.

[8] W. J. Van Dijck, *United States Patent* Nº 2814552A, 1957.

[9] P. E. Oberdorfer and R. F. Winch, "Chemicals from Methane in a high compression engine," *Industrial & Engineering Chemistry*, vol. 53, 41-44, 1961.

[10] I. Yamamoto, K. Kaneko, K. Kuwae, and K. Hiratsuka, "Production of synthesis gas by internal combustion engine," *Sixth World Petroleum Congress*, vol. 429, 1963.

[11] G. A. Karim, and N. P. Moore, "The production of synthesis gas and power in a compression ignition engine," *Journal of the Institute of Fuel*, vol. 105, 1963.

[12] G. Karim and N. Moore, "The production of hydrogen by the partial oxidation of Methane in a dual fuel engine," *SAE Technical Paper*, 1990.

[13] F. E. Lowther and W. M. Bohon, *United States Patent* Nº 4965052A, 1990.

[14] Dolinsky, J. L., Grunwald, V. R., Kolbanovsky, Y. A., Piskunov, S. E., Plate, N. A. & Tolchinsky, L. S. *Russia Patent* Nº 2096313C1, 1997.

[15] A. Schaller, N. Darvishsefat, and E. Schlucker, "Simulation and experimental investigation of labyrinth seals for reciprocating piston compressors," *Chemical Engineering & Technology*, vol. 41, 2018.

[16] L. Wang, J. Feng, M. Wang, Z. M. Ma, and X. Peng, "Leakage characteristic identification of labyrinth seals on reciprocating piston through transient simulations," *Mathematical Problems in Engineering*, vol. 2019, 2019.

[17] H. R. Kläy, "Reciprocating compressors with labyrinth pistons for Helium," *Cryogenics*, vol. 15, 569-571, 1975.

[18] K. Graunke and J. Ronnert, "Dynamic behavior of labyrinth seals in oilfree labyrinth-piston compressors," *International Compressor Engineering Conference*, 1984.

[19] F. Cangioli, Pennacchi, G. Vannini, L. Ciuchicchi, A. Vania, S. Chatterton, and P. Dang, "On the thermodynamic process in the bulk-flow model for the estimation of the dynamic coefficients of labyrinth seals," *Journal of Engineering for Gas Turbines and Power*, vol. 7A, 2017.

[20] F. Cangioli, P. Pennacchi, G. Vannini, and L. Ciuchicchi, "Effect of energy equation in one control-volume bulk-flow model for the prediction of labyrinth seal dynamic coefficients," *Mechanical Systems and Signal Processing*, vol. 98, 594-612, 2018.

[21] B. Hodkinson, "Estimation of the leakage through a labyrinth gland," *Proceedings of the Institution of Mechanical Engineers*, vol. 141, 283-288, 1939.

[22] L. M. Milne-Thomson, *Theorical hydrodynamics*, Courier Corporation, 1996.

[23] G. Vermes, "A fluid mechanics approach to the labyrinth seal leakage problem," *Journal of Engineering for Power*, vol. 83, 161-169, 1960.

[24] Glouchenkov, M., Kronberg, A., & Veringa, H. "Free Piston Pulsed Compression Reactor". *Chemical Engineering Transactions*, vol. 2, 983-988, 2002.

[25] H. E, Alcázar, B. R. Velasquez, A. Araujo de Morais Jr., L. O. Alcázar, "Numerical simulation of labyrinth seals for pulsed compression reactors (PCR)," *Proceedings of the XLI Ibero-Latin-American Congress on Computational Methods in Engineering*, ABMEC, CILAMCE, Foz do Iguaçu/PR, Brazil, November 16-19,2020.

[26] B. V. Encontech CTW, "Pulsed compression reactor for nanoparticles manufacturing," http://www.encontech.nl/papers/Nanoparticles%20 manufacturing.pdf

[27] ANSYS, Inc., "ANSYS Fluent Theory Guide, Section 4.3.3.1 Overview". *Ansys© Fluent*, Release 2020 R1,2020.

[28] ANSYS, Inc., "Ansys Customer Portal, Solutions: How to prescribe a target static pressure for a total pressure inlet condition using UDF?," *Ansys© Fluent*, Release 2019 R2, 2020.

[29] ANSYS, Inc., "ANSYS DesignXplorer User's Guide". *Ansys©*, Release 2020 R1,2020.

[30] W. Zhou, Z. Gan, X. Zhang, L. Qiu, and Y. Wu, "Clearance loss analysis in linear compressor with CFD method," *16th International Cryocooler Conference*, Cryocoolers 16, Atlanta, May 17-20, 2008.